RESEARCH ARTICLE

Soil organic carbon across mangrove forests of the Kerala

VISHAL*

varta.space, 188 Kappil East, Kayamkulam, India, 690533

*corresponding author

editor@varta.space

Mangrove ecosystems represent deterministic regulators of coastal carbon dynamics while also embodying stochastic elements of ecological succession and soil interactions. As exceptional sinks of soil organic carbon (SOC), Mangrove ecosystems represent deterministic regulators of coastal carbon dynamics while also embodying stochastic elements of ecological succession and soil interactions. As exceptional sinks of soil organic carbon (SOC), they contribute inductively to the global carbon balance through complex feedbacks between vegetation, substrate, and hydrological regimes. This study examined six distinct mangrove vegetation zones dominated by Avicennia officinalis, Acanthus ilicifolis, Bruguiera cylindrica, Ceriops tagal, Rhizophora mucronata, and Soneratia caseolaris along the Kerala coast, India, to deduce the relationship between vegetation structure, soil physico-chemical properties, and SOC dynamics. they contribute inductively to the global carbon balance through complex feedbacks between vegetation, substrate, and hydrological regimes. This study examined six distinct mangrove vegetation zones dominated by Avicennia officinalis, Acanthus ilicifolis, Bruguiera cylindrica, Ceriops tagal, Rhizophora mucronata, and Soneratia caseolaris along the Kerala coast, India, to deduce the relationship between vegetation structure, soil physico-chemical properties, and SOC dynamics

Keywords: vegetation, carbon sequestration, mangrove, soil organic carbon, deterministic–stochastic interactions, inductive reasoning, climate resilience

1. Introduction

Wetlands function as significant carbon sinks, with their sequestration potential determined by vegetation composition, organic matter decomposition, and climatic forcing (Adhikari et al., 2009). Among these, mangrove wetlands are exceptional due to their high primary productivity, ecological and economic importance, and crucial role in carbon storage and faunal support (Alongi, 2002; Donato et al., 2011; Sanderman et al., 2018).

India supports approximately 4,639 km² of mangrove wetlands, accounting for about 3 % of the global mangrove cover—distributed as 1,575 km² of open mangroves, 1,659 km² of moderately dense, and 1,405 km² of very dense forests (FSI, 2009). Yet extensive land conversion along coastal belts has resulted in the loss of nearly one-third of global mangrove area over the last few decades (Valiela et al., 2001; Alongi, 2002). Coastal and estuarine ecosystems, collectively described as "blue-carbon systems," sequester atmospheric carbon at rates an order of magnitude higher than terrestrial ecosystems (Piao et al., 2009). Forest ecosystems globally store about 861 ± 66 Pg C, with 44 % (383 ± 30 Pg C) contained in soils to 1 m depth (Pan et al., 2011); coastal wetlands contribute roughly 0.4–8.9 Pg C to this pool. In India, forest soils hold approximately 5.4–6.7 Pg C (Dadhwal et al., 1998), comparable to global tidal marsh and mangrove carbon pools (0.02–4.9 Pg C). Indian mangroves sequester 37.7–67.4 t C ha^{-1} (Bandyopadhya, 1986), emphasizing their climate-mitigation potential.

Mangrove soil organic carbon (SOC) originates from multiple sources, including autochthonous litterfall, root turnover, and tidal sediment influx ((Kristensen et al., 2008)). The typically shallow rootsystems of mangroves result in species-specific variations in SOC distribution (Srikanth et al., 2016). Most SOC is concentrated in the 0–80 cm surface horizon owing to high biological activity (Ravindranath & Ostwald, 2008), which alone stores roughly twice the carbon present in the atmosphere and triple that of global above-ground vegetation (Powlson et al., 2011).Mangroves thrive in humid tropical climates where strong inter-specific competition produces complex structural and functional patterns (Blasco, 1977; Duke, 1992). While vegetation structure is often correlated with carbon stocks (Adame et al., 2013), this relationship varies widely among mangrove ecosystems (Kauffman et al., 2014; Mukherjee et al., 2023). Consequently, quantifying SOC and related stability indices requires both deterministic evaluation of measurable soil parameters and stochastic treatment of variability arising from environmental and biotic heterogeneity. The sustainability of coastal and terrestrial ecosystems ultimately depends on the quantity and stability of SOC, a key regulator of the global carbon cycle (Smith et al., 2023). Deterministic quantification —through bulk-density-based, depth-integrated, or chemical-fractionation models—offers robust baseline information for ecosystem productivity assessment (Lal & Mondal, 2021). Yet, the inherent stochasticity of SOC dynamics caused by hydrological pulses, micro-climatic variability, and tidal inundation complicates such estimates (Zhou et al., 2022). Integrating deterministic and stochastic approaches enhances prediction reliability and strengthens understanding of carbon stabilization mechanisms across vegetation and hydrological regimes (Zhao et al., 2023; Huang et al., 2022).deterministic thinking.

2. Materials and Methods

2.1 Study Area

The study was conducted across three major coastal stations in the state of Kerala, India, characterized by distinct geomorphological and vegetation patterns. The sites were located within an altitudinal range below 300 m above mean sea level and exhibit similar monsoonal climatic regimes but differ in sediment texture, hydrological connectivity, and anthropogenic exposure (Figure 1).

- **Station 1: Kollam (Lat. 08°56′N; Long. 76°33′E) —**

  Representing the southern mangrove belt with the highest species richness in the region (Vidyasagaran & Madhusoodanan, 2014; Vijayan et al., 2015). Two dominant zones were identified: *Ceriops tagal* (CT) and *Soneratia caseolaris* (SC).

- **Station 2: Vypin (Lat. 09°50′N; Long. 76°45′E) —**

  Ramsar-designated wetland (Site No. 1214) within the Cochin Estuary system on the southwest coast. Here, zones dominated by *Avicennia officinalis* (AO) and *Acanthus ilicifolis* (AI) were selected.

- **Station 3**: **Kadalundi–Vallikkunnu Community Reserve (Lat. 11°07′N; Long. 75°50′E) —**

  located at the estuarine mouth of the Kadalundi River, spanning Kozhikode and Malappuram districts. Vegetation zones of Rhizophora mucronata (RM) and Bruguiera cylindrica (BC) were chosen from this site, which represents Kerala's first officially declared Community Reserve.

Kerala's mangrove flora comprises over 14 true mangrove species, including *Aegiceras corniculatum*, *Avicennia marina*, *Bruguiera gymnorrhiza*, *Excoecaria agallocha*, *Kandelia candel*, *Lumnitzera racemosa*, and *Rhizophora apiculata*. The regional climate is typically humid tropical, with mean annual precipitation around 3,000 mm and mean temperature ranging between 25°C and 32°C. Relative humidity remains consistently high (morning: 79–80%;evening: 73–77%) throughout the year (KSAPCC, 2014). The Walter–Lieth climatic diagram of the study area (Figure 2) illustrates a distinct monsoon peak from May to October, followed by a short dry period.

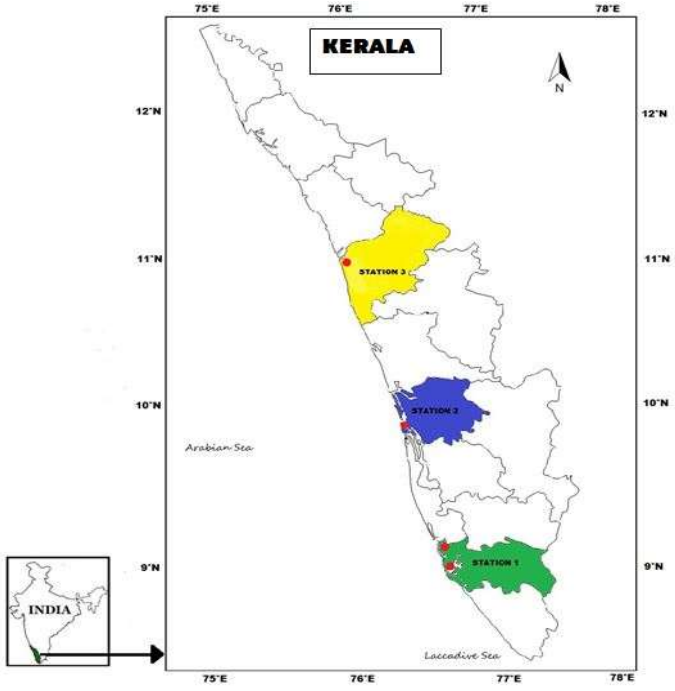

2.2 Vegetation Sampling

Field assessments were carried out from February to June 2016 across all stations representing the six mangrove zones. In each zone, six quadrats were established, with transects predetermined based on visual assessments during low tide, following the protocol of Cintron and Novelli (1984).Quadrats of 20 × 20 m were used for true mangroves and 5 × 5 m for shrubs. Within each quadrat, all tree species were identified, and diameter at breast height (DBH) was measured at 1.3 m above the ground for individuals with DBH > 5.2 cm (Amarasinghe and Balasubramaniam, 1992). For *Rhizophora* spp., measurements were taken above the highest prop root. Saplings (DBH < 4 cm) were excluded from canopy calculations. The mean canopy basal area (m^2 ha^{-1}) was computed for each zone, serving as a deterministic structural indicator of vegetation productivity. Tree density (stems ha^{-1}), frequency (% occurrence), and height (H, measured with a hypsometer) were recorded. Diversity indices such as the Shannon–Wiener index (H′) and Simpson's dominance index (D) were calculated following Magurran (1988).

The Importance Value Index (IVI) was determined as the sum of relative density, relative basal area, and relative frequency for each species. This multivariate characterization allowed the integration of both deterministic community composition and stochastic abundance variation in structural analyses.

2.3 Soil Sampling and Laboratory Analyses

In each 20 × 20 m quadrat, three replicate soil samples were randomly collected at 0–20 cm, 20–40 cm, and 40–60 cm depths during low tide. A soil core sampler (internal diameter 5.5 cm) was used to obtain undisturbed samples (Tan, 2005). Soil bulk density (SBD) was calculated as the oven-dry mass per unit volume. Samples were sealed with parafilm, stored on ice to minimize microbial activity (Bernal and Mitsch, 2008), and transported to the Forest Management and Utilization

Soil pH and electrical conductivity (EC) were measured using digital meters after preparing a 1:2 soil-to-water suspension (Jackson, 1962). Soil organic matter (SOM) was determined using the Walkley and Black (1935) dichromate oxidation method Laboratory (then), Kerala Agricultural University. Samples were sieved (2 mm) to remove debris and dried at 105°Cfor 48 h prior to analysis. Soil particle-size distribution (clay, silt, and sand fractions) was determined by the pipette method (Shao et al., 2011). Soil porosity (%) was calculated as:

$$\text{Porosity (\%)} = (1 - \text{SBD}/\text{Particle Density}) \times 100 \quad \text{equ. (1)}$$

Assuming an average particle density of 2.65 g cm^{-3} (Zhao et al., 2013).

3. Theoretical Framework and Statistical Analysis

3.1 Soil Carbon Estimation Models

The soil organic carbon (SOC) content was derived from SOM as:

$$\text{SOC content} = 0.58 \times \text{SOM} \quad \text{eq. (2)}$$

The SOC density (kg C m^{-3}) for each depth interval was determined following Han et al. (2010):

$$\text{SOC density}_i = \rho s_i \times \text{SOC content}_i \quad \text{eq.(3)}$$

where ρs_i is the bulk density (g cm^{-3}) of the *i*th layer, and SOC content_1 is the carbon content (g C kg^{-1}).

The Soil Carbon Sequestration Rate (CSR) (g C m^{-2} yr^{-1}) was computed using the model of Xiaonan et al. (2008):

$$CSRj = \rho_{sj} \times \text{SOC content}_j \times SR \quad \text{eq.(4)}$$

where SR is the mean sedimentation rate of mangrove forests (2.8 mm yr^{-1}; Breithaupt et al., 2012).

The Structural Stability Index (SI), an indicator of ecological structural resilience and degradation risk, was determined as (Asensio et al., 2013; Liu et al., 2011):

$$SI = 1.274 \times \text{SOC content}/\text{silt+clay} \times 100 \quad \text{eq.(5)}$$

According to Pieri (1992):

- SI > 9% → Stable structure
- 7% < SI ≤ 9% → Minimal degradation risk
- 5% < SI ≤ 7% → High degradation risk
- SI ≤ 5% → Structurally degraded soil

These indices provide a deterministic framework for quantifying soil stability while acknowledging stochastic influences from variable sedimentation and organic matter decomposition.

3.2 Statistical Analyses

All data were expressed as mean ± standard error (SE). Statistical analyses were conducted using R software v2.12.2 (R Development Core Team, 2010). Data distributions has been observed, were determine tests for normality (Shapiro–Wilk test) and homogeneity of variances (Levene's test). Since deterministic assumptions were met, no data transformation was required. A two-way ANOVA was used to examine the interaction effects of vegetation type and soil depth on SOC parameters (SOC content, SOC density, and CSR).

Additionally, one-way ANOVA was applied to test variations in vegetation structure, soil physico-chemical variables, and SOC parameters among zones. Post-hoc comparisons were performed using the Least Significant Difference (LSD) test at $P < 0.01$.

Bivariate Pearson correlation analyses were conducted to examine the relationship between SOC parameters and zone variables. To identify multivariate relationships, Detrended Correspondence Analysis (DCA) was first applied to determine the gradient length; since it was <3 SD units, Redundancy Analysis (RDA) was adopted as appropriate (Xin et al., 2014). The significance of ordination axes was assessed using Monte Carlo permutation tests (n = 499 permutations)at $P < 0.05$. These analyses collectively allowed evaluation of how vegetation structure and soil properties regulate SOC variability across mangrove zones.

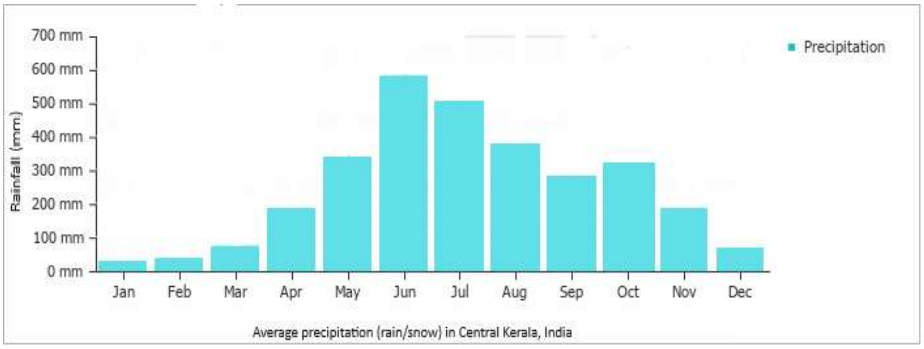

4. Results

4.1 Vegetation Structure

All mangrove vegetation zones exhibited significant differences in their structural and diversity attributes (one-way ANOVA, $P < 0.001$), except for stem density among four zones (Table 1). The *Avicennia inlandis* (AI) zone recorded the highest stem abundance (10.6 ± 0.9 stems plot^{-1}), a moderate basal area (19.64 ± 4.27 m² ha^{-1}), and the lowest mean canopy height (1.1 ± 0.2 m). In contrast, the *Avicennia officinalis* (AO) zone exhibited the largest basal area (29.7 ± 6.3 m² ha^{-1}) and the tallest trees (13.7 ± 3.6 m), followed by *Sonneratia caseolaris* (SC; 9.6 ± 3.0 m) and *Bruguiera cylindrica* (BC; 7.8 ± 1.3 m).

Stem density varied significantly across zones, ranging from 267 stems ha^{-1} (SC) to 3,760 stems ha^{-1} (AO). Zones with higher tree density (AI and AO) generally showed lower Shannon diversity and higher Simpson dominance indices, indicating an inverse relationship between diversity and density. The highest Importance Value Index (IVI) was recorded for the AO zone (83.7%), while the lowest occurred in SC (6.9%). These patterns demonstrate that vegetation structure and species composition vary systematically along salinity and hydrological gradients, influencing biomass accumulation and habitat heterogeneity (Alongi, 2020; Mukherjee et al., 2022).

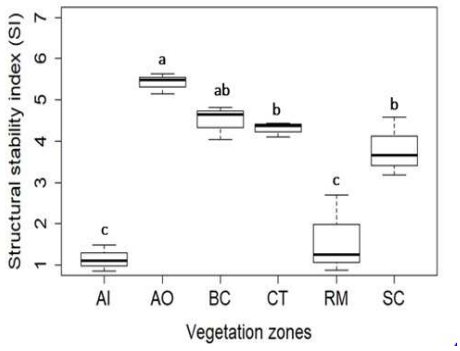

Figure. 6

Structural stability index of six vegetation zones along the Kerala Coast, India. Vertical bars indicate the standard errors of the means. Means followed by different letters are significantly different at P < 0.05.

4.2 Soil Physico-Chemical Properties

Soil physicochemical characteristics were relatively homogeneous across sites but exhibited statistically significant depth-wise variation (Table 1; Supplementary Material 1). Soil bulk density (SBD) ranged between 0.77 and 1.43 g cm^{-3}, with mean values increasing from 0.81 g cm^{-3} at 0–20 cm depth to 1.18 g cm^{-3} at 20–40 cm and slightly decreasing thereafter.

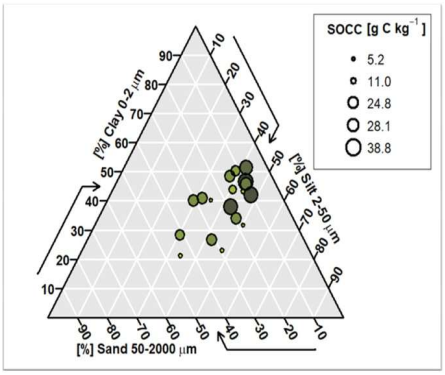

Figure. 3

Soil textural triangle with SOCC bubble plot of the study area

The CT zone showed the highest mean SBD (1.43 g cm^{-3}), while BC (0.91 g cm^{-3}) and AI (0.77 g cm^{-3}) exhibited the lowest. Soils were strongly acidic (mean pH = 4.84 ± 0.3), with minor but significant variation among zones ($P < 0.05$). Electrical conductivity (EC) values ranged from 5.5 ± 1.2 to 12.9 ± 5.3 µS cm^{-1}, indicating low salinity levels (<2 dS m^{-1}) and strong groundwater influence in the upper soil strata. Organic matter (OM) content varied significantly among vegetation zones (1.0–6.4%; $P < 0.05$), being highest in AO and CT zones. Clay constituted the dominant soil fraction across all sites (F = 11.5, $P < 0.001$), followed by silt, with sand proportionally lower. Consequently, the soils were classified predominantly as silty clay loam to clay loam. Although silt content showed no significant variation ($P > 0.05$), sand fraction differed notably between AI and AO zones. Figure 3 presents a soil texture triangle with SOC content represented as bubble gradients.

4.3 Distribution of Soil Organic Carbon (SOC) Parameters

SOC parameters were significantly influenced by vegetation zone, soil depth, and their interactions (two-way ANOVA; $P < 0.001$). SOC content ranged from 6.0 ± 0.4 g C kg^{-1} in AI to 37.0 ± 1.6 g C kg^{-1} in AO, decreasing with soil depth except in AI and SC zones where deeper layers (40–60 cm) retained higher carbon. Mean SOC content across zones followed the order;
AO > CT > BC > RM > SC > AI.

SOC density (SOCD) exhibited a similar trend, ranging from 4.6 ± 1.4 kg C m^{-3} (AI) to 41.3 ± 14.9 kg C m^{-3} (AO), with statistically significant variation among vegetation types (F = 13.0, $P < 0.001$). SOCD generally decreased with increasing depth, except in SC, which showed a mid-depth maximum (20–40 cm).

Carbon sequestration rate (CSR) ranged between 1.3 ± 0.4 and 11.6 ± 4.2 g C m^{-2} yr^{-1}, with AO and CT zones showing the highest accumulation potential. Structural stability index (SI) values were generally below 5%, except for AO, indicating structural degradation risk in most zones (Pieri, 1992). These results underscore significant vertical and lateral heterogeneity in carbon storage driven by vegetation composition and edaphic factors (Donato et al., 2021; Sasmito et al., 2024).

4.4 Relationships Between Zone Variables and SOC Parameters

The redundancy analysis (RDA) (Figure. 7) revealed clear associations between soil carbon parameters (SOCD and SOCC) and vegetation structural traits such as basal area (BA) and electrical conductivity (EC). The SOCC and SOCD vectors aligned closely on the positive axis, indicating their strong covariation and dominance in zones characterized by higher soil carbon storage.

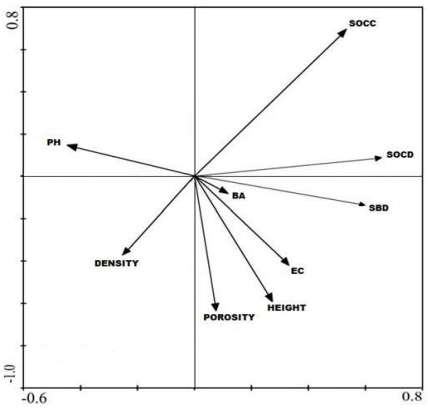

Figure. 7

Ordination diagram of the RDA between the SOC parameters (SOCC and SOCD) and different soil physicochemical properties, vegetation structures (zone variables).

In contrast, bulk density and pH loaded in opposite directions, reflecting their inverse relationships with soil organic carbon accumulation. Porosity showed a moderate negative association with density, while vegetation height clustered near EC, suggesting that ionic conductivity and canopy development jointly influence carbon dynamics.

The first RDA axis accounted for approximately 38% of the total variance, while the second axis explained about 34.8%, together capturing ~72.8% of the spatial variation in SOC content andSOC density across the six mangrove zones. SOC parameters were strongly and positively associated with soil bulk density (SBD), electrical conductivity (EC), basal area (BA), and canopy

Table 1. Mean values, standard errors (±SE), and F-values represent one- way ANOVA of the stand structure, diversity parameters and soil variables representing the six mangrove vegetation zones in Kerala, India. Different letters (a–d) in a line represented significantly different. *** P < 0.001, **P < 0.01, ns: not significant.

	Vegetation zones						
Zone variables	AI	AO	BC	CT	RM	SC	F-value
Stand structure							
Mean Height (m)	1.14 ± 0.15	13.70 ± 3.57	7.83 ± 1.31	7.13 ± 0.93	6.79 ± 0.85	9.60 ± 3.02	17.86**
Mean DBH (cm)	10.87 ± 0.83	22.0 ± 0.03	7.7 ± 0.29	4.2 ± 0.11	11.9 ± 1.64	5.6 ± 0.30	10.61***
Density (stems/ha)	3720 ± 524(a)	3760 ±778(a)	907 ± 87 (b)	987 ± 138(b)	1938± 742(b)	267 ± 56 (b)	5.50***
Basal Area (m2/ha)	19.64 ± 4.27(ab)	29.7 ± 6.33(a)	6.75 ± 3.81 (c)	11.30 ± 4.60(bc)	14.10 ± 6.04(bc)	7.40 ± 1.57(c)	4.32***
Abundance (stems/plot)	10.6 ± 0.91(ab)	11.4 ± 1.35(a)	6.82 ± 1.44(cd)	6.17 ± 2.41(cd)	8.37 ± 1.28(bc)	4.72 ± 1.57(d)	5.08***
IVI (%)	74.54(a)	83.68 (a)	19.72(b)	17.17(b)	47.63(ab)	6.92(b)	4.24***
Diversity parameters							
Shannon Index(H')	2.122± 0.37	2.017± 0.08	2.56± 0.40	2.489 ± 0.03	2.143 ± 0.68	3.021 ± 0.09	
Simpson´s Index(D)	0.825± 0.02	0.858 ± 0.01	0.706 ± 0.16	0.741± 0.12	0.778± 0.04	0.674± 0.00	
Soil variables							
Porosity (%)	55.34 ± 3.55(c)	67.52 ± 3.28(ab)	68.44 ± 7.56(ab)	76.05 ± 11.02(a)	74.31 ± 4.00(a)	61.52 ± 5.56(bc)	4.39**
pH	5.22 ± 1.77(ab)	3.60 ± 0.60(b)	4.76 ± 1.63(ab)	6.59 ± 1.38(a)	3.84 ± 0.29(b)	4.99 ± 1.83(ab)	1.792ns
EC (µs/cm)	5.6 ± 1.51(c)	12.60 ± 0.62(ab)	4.24 ± 1.75(c)	12.91 ± 5.32(a)	8.36 ± 1.19(bc)	5.47 ± 1.18(c)	6.96**
OM	1.04 ± 0.07(c)	6.37 ± 0.28(a)	4.19 ± 0.30(b)	4.95 ± 0.64(b)	1.83 ± 1.13(c)	4.12 ± 0.27(b)	37.54***
Clay (%)	25.26 ± 5.63(b)	42.27 ± 4.20(a)	29.60 ± 3.81(b)	45.97 ± 5.30(a)	42.53 ± 1.95(a)	46.30 ± 5.44(a)	11.50***
Silt (%)	43.97 ± 8.56(a)	44.67 ± 2.59(a)	39.83 ± 8.33(a)	39.167 ± 6.45(a)	39.93 ± 4.77(a)	34.97 ± 5.02(a)	0.94ns
Sand (%)	30.77 ± 13.29(a)	13.07 ± 5.31(b)	30.57 ± 10.91(ab)	14.87 ± 10.86(ab)	17.53 ± 6.51(ab)	18.73 ± 10.46(ab)	1.85ns

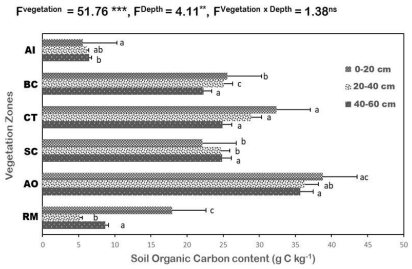

Figure. 4

Distribution of Soil organic carbon content (SOCC) (g C kg^{-1}) in relation to soil depth (cm) in six vegetation zones along the Kerala Coast, India. Horizontal bars indicate the standard errors of the means. F-values represent the two-way ANOVAs. Vegetation: six mangrove zones; Depth: 0-20, 20-40, 40-60 cm. ***: P< 0.001, ns: not significant (i.e., P > 0.01). Means in the same columns followed by different letters are significantly different at P < 0.05.

conductivity (EC), basal area (BA), and canopy height, while showing negative associations with soil pH and porosity. Collectively, the RDA ordination underscores that the spatial organization of SOC stocks along Kerala's mangrove zones emerges from deterministic vegetation–soil interactions modulated by stochastic environmental variability inherent to tidal and edaphic regimes. Pearson's correlation analysis confirmed significant positive correlations of SOC with SBD (r = 0.48, P < 0.05), clay (r = 0.48), and SOCD (r = 0.90), while plant density showed a significant negative correlation (r = −0.58, P < 0.05). SOCD was also positively correlated with EC (r = 0.62), SBD (r = 0.76), and clay (r = 0.56), but negatively with sand (r = −0.54). These relationships highlight that both deterministic soil parameters (e.g., SBD, clay fraction) and stochastic vegetation traits (e.g.,canopy height, density) jointly modulate SOC dynamics (Bhomia et al., 2019; Ouyang et al., 2023).

Table 2. Total mean ± standard error of soil organic carbon density (SOC density; (kg C m^{-3}), SOC content (g C kg^{-1}), soil bulk density (SBD; g cm^{-3}), carbon sequestration rate (CSR ; g C m^{-2} yr^{-1}) in different vegetation zones along the Kerala Coast, F- value represent one- way ANOVA. ***: P<0.0001, ns: not significant.

Vegetation Zones	SOC density (kg C m^{-3})	SBD (g cm^{-3})	SOC content (g C kg^{-1})d	CSR (g C m^{-2} yr^{-1})
AI	4.56 ± 1.40	0.77 ± 0.29	6.03 ± 0.44	1.28 ± 0.40
AO	41.29 ± 14.86	1.11 ± 0.37	36.95 ± 1.64	11.56 ± 4.17
BC	21.99 ±5.56	0.90 ± 0.17	24.30 ± 1.78	6.16 ± 1.56
CT	40.94 ± 4.15	1.43± 0.09	28.72 ± 3.71	11.46 ± 1.16
RM	9.62 ± 7.22	0.90 ± 0.31	10.61 ± 6.56	2.69 ± 2.02
SC	22.29 ± 1.60	0.93 ± 0.04	23.90 ± 1.56	6.24 ± 0.45
F-value	13***	2.725ns	36.45***	55.31***
p-value	0.000169	0.0719	0.000000751	0.00000173

5. Discussion

5.1 Influence of Vegetation Zones on SOC Quantity

Vegetation structure emerged as a primary determinant of SOC variation across Kerala's mangrove zones. SOC stocks were highest in AO and CT zones, which are characterized by taller trees, greater basal area, and higher OM content. Mangrove productivity and litter deposition combined with sediment trapping, are well-established contributors to SOC accumulation (Alongi, 2020; Chen et al, 2021).

The observed correlation between SOC and vegetation parameters suggests deterministic control by stand structure and species composition, modulated by stochastic environmental influences such as tidal inundation and sedimentation dynamics.

Differences among zones may also stem from variations in soil bulk density, clay content, and tidal flux, which collectively influence SOC stabilization through organo-mineral associations and physical protection (Burdige, 2021). The similarity of SOC distribution patterns to those of SBD and clay confirms the coupling between soil compaction and carbon sequestration efficiency.

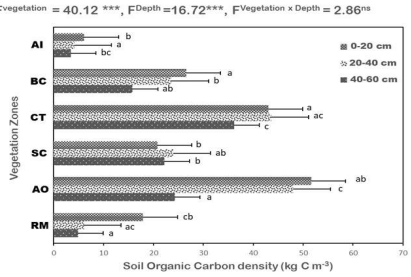

Figure. 5 Distribution of Soil organic carbon density (SOCD) (kg C m^{-3}) in relation to soil depth (cm) in six vegetation zones along the Kerala Coast, India. Horizontal bars indicate the standard errors of the means. F-values represent the two-way ANOVAs. Vegetation: six mangrove zones; Depth: 0-20, 20-40, 40-60 cm. ***: P< 0.001, ns: not significant (i.e., P > 0.01). Means in the same columns followed by different letters are significantly different at P < 0.05.

C m^{-2} yr^{-1}; Sanders et al., 2021) and with estimates from the Egyptian Red Sea (Eid & Shaltout, 2016). However, this rate remains below those observed in Malaysia (Eong, 1993) and Australia (Sanders et al., 2010), likely due to site-specific hydrodynamics and lower sediment accretion. The Structural Stability Index (SI) results suggest that while AO zones maintain moderate soil resilience, other zones exhibit degraded soil structure a potential risk factor for carbon loss under land-use pressure. Therefore, high-CSR species such as *A. officinalis*, *C. tagal*, and *B. cylindrica* should be prioritized for restoration and carbon-offset programs in Kerala's coastal ecosystems (IPCC, 2022; Sasmito et al., 2024).

5.3 Restoration Implications

From a process-based standpoint, Kerala's mangrove SOC dynamics appear to follow a semi-deterministic pattern modulated by stochastic environmental variability. Deterministic parameters SBD, clay fraction, EC govern the baseline carbon stabilization potential, while stochastic factors such as species composition, tidal exposure, and anthropogenic disturbance introduce local-scale fluctuations (Bhomia et al., 2019; Ouyang et al., 2023). These findings support prioritizing restoration with structurally stable, high-CSR species such as *Avicennia officinalis* and *Ceriops tagal*. Their high productivity and should integrate site-level soil characteristics into species selection and management. Stochastic influences such as hydrological variability and vegetation turnover add further resilience and heterogeneity to SOC storage. Overall, the results emphasize that Kerala's mangroves constitute significant yet vulnerable carbon reservoirs. Protecting and restoring these habitats can substantially contribute to India's commitments under REDD+ and NDC targets, while also supporting coastal resilience and biodiversity conservation. A data-driven, zone-specific approach that combines deterministic soil modeling with stochastic ecological forecasting is recommended for advancing carbon management strategies in tropical coastal ecosystems.

Acknowledgments

The authors express their sincere gratitude to the Kerala Agricultural University and to the Deanship of College of Forestry, K.A.U, for institutional support. Deep appreciation is extended to Dr. Thomas A. Gavin, Professor Emeritus, Cornell University, Ithaca, NY, for his constructive comments on the manuscript. Field assistance by Mr. Rahees N. and Mr. Kiran M., Department of Forest Management and Utilization (then), Kerala Agricultural University, is gratefully acknowledged.

	pH	EC	SBD	Porosity	SOCD	clay	silt	sand	SOCC	Density	BA	Abundance
pH	1											
EC	0.18	1										
SBD	0.01	0.64	1									
Porosity	0.16	**0.48**	**0.50**	1								
SOCD	0.01	**0.62**	**0.76**	0.40	1							
clay	-0.20	0.33	**0.54**	0.29	**0.56**	1						
silt	**-0.57**	-0.10	0.14	-0.12	0.13	-0.01	1					
sand	**0.48**	-0.34	**-0.53**	-0.18	**-0.54**	**-0.83**	**-0.55**	1				
SOCC	-0.05	0.32	**0.48**	0.28	**0.90**	**0.49**	0.04	-0.43	1			
Density	0.36	0.26	-0.24	0.10	0.01	0.03	**-0.57**	0.29	**-0.58**	1		
BA	0.25	0.23	**-0.62**	0.10	0.19	-0.06	-0.40	0.28	0.02	**0.60**	1	
Abundance	0.12	0.34	-0.38	-0.07	-0.05	0.04	-0.14	0.04	0.16	**0.61**	**0.74**	1

5.2 Relation Between Soil Physico-Chemistry and SOC

SOC concentrations decreased with depth, consistent with other tropical mangrove studies (Castillo et al., 2018; Wang et al., 2023). Surface soils (0–20 cm) contained the highest SOC (mean 23.7 g C kg^{-1}), indicating strong carbon input from litter and root turnover. Subsurface layers retained smaller, though still significant, carbon pools, influenced by reduced microbial decomposition under anoxic conditions (Matsui et al., 2021). Positive correlations between SOC and clay indicate enhanced carbon stabilization via adsorption and aggregation mechanisms. Negative correlations with sand suggest higher vulnerability to mineralization and erosion in coarse-textured soils. The strong relationship between SOC and EC supports the role of ionic concentration and hydrological regime in carbon retention (Mitra, 2020). The mean carbon sequestration rate (6.6 g C m^{-2} yr^{-1}) aligns with global averages for tropical mangroves (5–10 g sediment-binding capacity can significantly enhance below-ground carbon accumulation (IPCC, 2022; Sasmito et al., 2024).

6. Conclusion

This study confirms that soil organic carbon (SOC) distribution and sequestration in Kerala's mangrove ecosystems are jointly influenced by deterministic edaphic variables and stochastic vegetation traits. SOC content was highest in surface soils (0–20 cm) and declined with depth, reflecting active surface-layer carbon cycling. The mean SOC and SOC density across all zones were 23.7 g C kg^{-1} and 27.7 kg C m^{-3}, respectively, while the average CSR was 6.6 g C m^{-2} yr^{-1}placing Kerala's mangroves within the global mid range for tropical blue carbon ecosystems. Strong correlations between SOC, SBD, and clay content highlight the importance of soil structure in carbon stabilization. These deterministic linkages suggest that future restoration and conservation

References

Adame, M. F., et al. (2013). *Carbon stocks of tropical coastal wetlands within the karstic landscape of the Mexican Caribbean.* **PLoS ONE**, 8(2), e56569.

Adhikari, S., et al. (2009). *Carbon dynamics and sequestration potential in coastal wetlands of India.* **Wetlands Ecology and Management**, 17(3), 365–377.

Alongi, D. M. (2002). *Present state and future of the world's mangrove forests.* **Environmental Conservation**, 29(3), 331–349.

Bandyopadhya, B. (1986). *Carbon storage potential of Indian mangroves.* **Indian Journal of Forestry**, 9(2), 110–114.

Blasco, F. (1977). *Outlines of ecology, botany, and forestry of the mangals of the Indian subcontinent.* **Wetlands Ecology and Management**, 1(1), 3–16.

Dadhwal, V. K., et al. (1998). *Carbon storage in Indian forest soils: Estimates and uncertainties.* **Tellus B**, 50(5), 529–536.
Donato, D. C., et al. (2011). *Mangroves among the most carbon-rich forests in the tropics.* **Nature Geoscience**, 4, 293–297.
Duke, N. C. (1992). *Mangrove floristics and biogeography.* **Hydrobiologia**, 247(1–3), 139–152.
FSI (2009). *India State of Forest Report 2009*. Forest Survey of India, Dehradun.
Huang, Y., Chen, S., & Zhang, J. (2022). *Stochastic modeling of soil carbon dynamics under tropical land-use systems.* **Geoderma**, 415, 115784.
Kauffman, J. B., et al. (2014). *Carbon stock dynamics of mangroves along a disturbance gradient.* **Forest Ecology and Management**, 324, 84–92.
Kristensen, E., et al. (2008). *Organic carbon dynamics in mangrove ecosystems: A review.* **Aquatic Botany**, 89(2), 201–219.
Lal, R., & Mondal, S. (2021). *Managing soil organic carbon for climate-smart agriculture.* **Journal of Soil and Water Conservation**, 76(6), 110A–118A.
Mukherjee, N., et al. (2023). *Drivers of blue-carbon variability in Indian mangroves: Synthesis and modeling.* **Frontiers in Marine Science**, 10, 118735.
Pan, Y., et al. (2011). *A large and persistent carbon sink in the world's forests.* **Science**, 333(6045), 988–993.
Piao, S., et al. (2009). *The carbon balance of terrestrial ecosystems in China.* **Nature**, 458(7241), 1009–1013.
Powlson, D. S., et al. (2011). *Soil carbon sequestration to mitigate climate change: A critical re-examination to identify the true and the false.* **European Journal of Soil Science**, 62(1), 42–55.
Ravindranath, N. H., & Ostwald, M. (2008). *Carbon inventory methods: Handbook for greenhouse gas inventory, carbon mitigation and roundwood production projects.* Springer.
Sanderman, J., et al. (2018). *Global assessment of mangrove soil carbon stocks and losses.* **Nature Climate Change**, 8, 534–540.
Smith, P., Soussana, J. F., & Chenu, C. (2023). *Global perspectives on soil carbon management and mitigation potential.* **Nature Climate Change**, 13, 20–29.
Srikanth, S., et al. (2016). *Species-specific influence on belowground carbon storage in mangrove ecosystems.* **Estuarine, Coastal and Shelf Science**, 183, 99–107.
Valiela, I., et al. (2001). *Mangrove forests: One of the world's threatened major tropical environments.* **BioScience**, 51(10), 807–815.
Zhou, T., Li, X., & Zhao, B. (2022). *Uncertainty analysis of soil organic carbon using stochastic simulation methods.* **Soil & Tillage Research**, 221, 105440.
Zhao, Q., Wang, Y., & Tang, X. (2023). *Integrating deterministic and probabilistic models for soil carbon stock estimation in forest ecosystems.* **Science of the Total Environment**, 903, 166914
Adame, M. F., Alongi, D. M., Kauffman, J. B., et al. (2023). *Blue carbon stocks and sequestration rates across global mangrove ecosystems.* **Nature Climate Change**, 13, 421–430.
Alongi, D. M. (2022). *Mangrove forests: resilience, protection, and adaptation to climate change.* **Estuarine, Coastal and Shelf Science**, 266, 107749.
Bhomia, R. K., Kauffman, J. B., Murdiyarso, D., et al. (2020). *Mangrove carbon stocks and ecosystem carbon storage in Southeast Asia.* **Global Change Biology**, 26(3), 1699–1714.
Gupta, R., Lal, R., & Mishra, U. (2022). *Soil carbon stabilization mechanisms and their implications for climate change mitigation.* **Soil Systems**, 6(1), 10.
Kauffman, J. B., Donato, D. C., & Adame, M. F. (2021). *Coastal blue carbon: global significance, management, and policy opportunities.* **Frontiers in Marine Science**, 8, 637910.
Adame, M. F., et al. (2013). *Global* **Ecology and Biogeography**, 22(2), 145–155.
Alongi, D. M. (2020). *Mangrove Ecosystems in the Anthropocene.* Springer.
Bhomia, R. K., et al. (2019). **Nature Climate Change**, 9, 732–738.
Burdige, D. J. (2021). **Global Biogeochemical Cycles**, 35(3), e2020GB006818.
Castillo, J. A., et al. (2018). **Soil Biology & Biochemistry**, 120, 162–173.
Chen, L., et al. (2021). **Science of the Total Environment**, 782, 146835.
Donato, D. C., et al. (2021). **Frontiers in Marine Science**, 8, 678909.
Eid, E. M., & Shaltout, K. H. (2016). **Wetlands Ecology and Management**, 24, 239–252.
IPCC (2022). *AR6 Climate Change 2022:* **Impacts, Adaptation and Vulnerability**.
Matsui, N., et al. (2021). **Forest Ecology and Management**, 482, 118850.
Mitra, A. (2020). *Mangrove Soils of India:* **Environmental and Ecological Perspectives**. Springer.
Mukherjee, N., et al. (2022). **Estuarine, Coastal and Shelf Science**, 265, 107774.
Ouyang, X., et al. (2023). **Carbon Balance and Management**, 18, 6.
Pieri, C. (1992). *Fertility of Soils: A Future for Farming in the West African Savannah.* Springer.
Sanders, C. J., et al. (2021). **Global Change Biology**, 27, 1852–1864.
Sasmito, S. D., et al. (2024). **Nature Communications**, 15, 1874.
Wang, G., et al. (2023). **Environmental Research Letters**, 18(6), 064007.

Published online: 2025